Available online at www.sciencedirect.com

SciVerse ScienceDirect

Ceramics International 39 (2013) 4569–4574

CERAMICS INTERNATIONAL

www.elsevier.com/locate/ceramint

Application of Zn_2SnO_4 photocatalyst prepared by microwave-assisted hydrothermal route in the degradation of organic pollutant under sunlight

Edson Luiz Foletto[a,*], Jana Marimon Simões[a], Marcio A. Mazutti[a], Sérgio L. Jahn[a], Edson Irineu Muller[b], Letícia Severo Fagundes Pereira[b], Erico Marlon de Moraes Flores[b]

[a]Department of Chemical Engineering, Federal University of Santa Maria, 97105-900 Santa Maria, Brazil
[b]Department of Chemistry, Federal University of Santa Maria, 97105-900 Santa Maria, Brazil

Received 5 October 2012; received in revised form 19 November 2012; accepted 19 November 2012
Available online 30 November 2012

Abstract

Zn_2SnO_4 crystals were successfully synthesized under microwave-assisted irradiation. The structural properties of the powders were investigated by X-ray diffraction (XRD) and N_2 adsorption/desorption isotherms (BET). Through a microwave-assisted hydrothermal route, porous Zn_2SnO_4 particles with a high specific surface area were obtained in a short synthesis time. In addition, Zn_2SnO_4 particles were tested as a photocatalyst for the degradation of textile dye under sunlight. The results showed that the maximum photocatalytic activity of Zn_2SnO_4 particles was about 50% degradation of the Reactive Red 141 dye in 270 min under sunlight irradiation, and that photocatalytic process followed zero-order kinetics. After sunlight exposure, 37% of total organic carbon (TOC) was removed. The photocatalytic results indicated that the Zn_2SnO_4 particles can be promising in the degradation of dye from aqueous solution under sunlight.

Keywords: Zn_2SnO_4; zinc stannate; Microwave-hydrothermal; Photocatalysis

1. Introduction

As an important member of transparent semiconductor materials, zinc stannate (Zn_2SnO_4) is known to have high electrical conductivity, high electron mobility and low visible absorption [1,2], which makes it suitable for a wide range of applications, such as gas-sensing material [3], anode material for Li-ion batteries [4], adsorbent for the dye removal [5] and as a photocatalyst for degradation of benzene [6] and also dye [7] from aqueous solution. The formation of Zn_2SnO_4 phase has been obtained by different routes such as solid-state reaction [8], mechanical and thermal activation [9], co-precipitation [10], thermal evaporation [11], vapor chemical deposition [12], synthesis using supercritical water in a bath reactor [13] and hydrothermal synthesis [14]. The microwave-assisted hydrothermal method has been used for the synthesis of inorganic nanoparticles [15,16]. Compared to other methods, the microwave-assisted hydrothermal method is simpler, faster and economic [16]. Although the synthesis Zn_2SnO_4 is well reported in literature, to the best of our knowledge, this is the first report focusing the microwave-assisted hydrothermal process for the synthesis of Zn_2SnO_4 particles for application in the field of the photocatalysis.

In this context, the main objective of this work was to synthesize Zn_2SnO_4 particles by the microwave-assisted hydrothermal method and to demonstrate their potential on the degradation of textile dye from aqueous solution under sunlight. The particles were characterized by X-ray diffraction (XRD) and surface area (BET).

2. Experimental

2.1. Synthesis and characterization of the Zn_2SnO_4 spinel

Zinc acetate ($ZnAc_2 \cdot 2H_2O$, analytical grade) and tin tetrachloride ($SnCl_4 \cdot 5H_2O$, analytical grade) were used as zinc and tin sources respectively without further purification. The zinc acetate aqueous solution (25.7 g in 115 mL) was added into tin tetrachloride aqueous solution (17.6 g

*Corresponding author. Tel.: +55 55 32208448; fax: +55 55 32208030.
E-mail address: efoletto@gmail.com (E.L. Foletto).

0272-8842/$ - see front matter © 2012 Elsevier Ltd and Techna Group S.r.l. All rights reserved.
http://dx.doi.org/10.1016/j.ceramint.2012.11.053

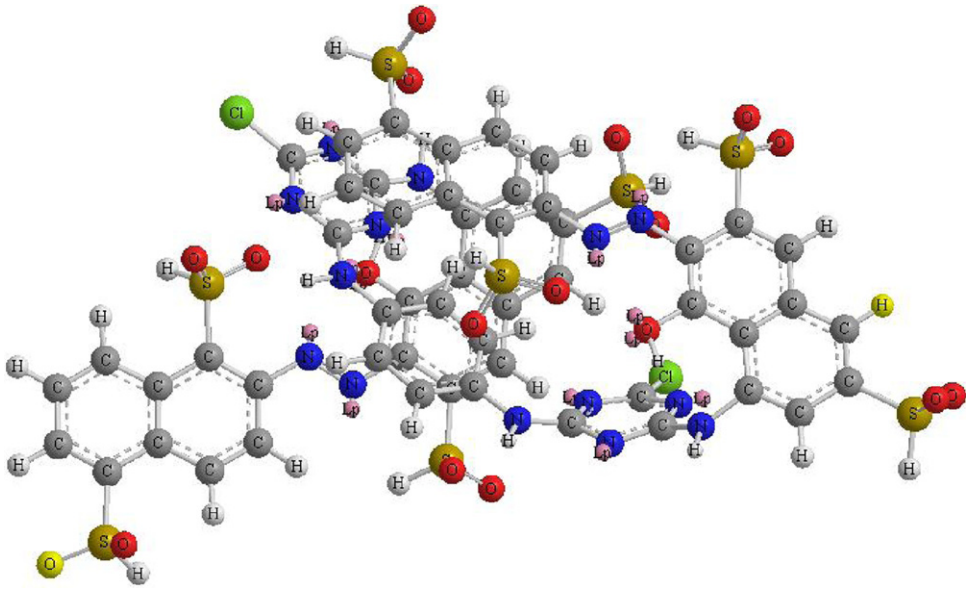

Fig. 1. Three dimensional chemical structure of Reactive Red 141 dye, obtained from ChemBio 3D Ultra version 11.0 program.

in 100 mL) slowly. Sodium hydroxide solution, (5 mol L^{-1}) used as mineralizer, was added dropwise into the mixture under magnetic stirring, until pH 7.5. The final mixture was charged into a microwave oven (Multiwave 3000 microwave sample preparation system, Anton Paar, Graz, Austria) equipped with eight high-pressure quartz vessels. The internal volume of vessels was 80 mL and the maximum operational temperature and pressure were set at 250 °C and 60 bar, respectively. The microwave-heating program was started by applying (i) 1000 W with a ramp of 5 min, (ii) 1000 W for 5 min, and (iii) 0 W for 20 min (cooling step). The procedures (i and iii) were similar for the reaction times of (ii) 10, 20 and 30 min. The precipitate was filtered, washed with distilled water, and dried at 100 °C for 10 h.

Powder was characterized by X-ray diffractometry (XRD; Bruker D8 Advance, with Cu Kα radiation, $\lambda = 0.15405$ nm). N_2 adsorption–desorption isotherm measurements were carried out at 77 K using an ASAP 2020 apparatus, at a relative pressure (P/Po) from 0 to 0.99.

2.2. Photocatalytic tests

The photocatalytic experiments were carried out under sunlight in a glass vessel ($Ø_{int} = 10$ cm) from 11.00 am to 3.30 pm during the month of march/2012 (summer season) at Santa Maria City (29°43′23″S and 53°43′15″W), Brazil. Schematic diagram of experimental apparatus was demonstrated in a previous study [17]. The photocatalytic degradation of textile dye Reactive Red 141 (RR141) (CAS number 61931-52-0; chemical formula is $C_{52}H_{34}O_{26}S_8Cl_{12}N_{14}$; molecular weight = 1952 g mol^{-1}; see the chemical structure in Fig. 1) was studied using a dye concentration of 150 mg L^{-1}. Prior to sunlight irradiation, the suspension containing the dye and the photocatalyst (dye solution/catalyst ratio = 1.0 g L^{-1}) was magnetically stirred for 45 min in dark to establish the adsorption equilibrium. Afterwards, the dye solution (200 mL) was stirred with a magnetic stirrer under sunlight and aliquots were taken at certain periods of time. These aliquots were centrifuged before the analysis of color. The concentration of dye in aqueous solution was determined by spectrometry (Spectro vision T6–UV model) at $\lambda_{máx} = 545$ nm. The photocatalytic degradation performance of the process was defined as % degradation $= (A_0 - A)/A_0 \times 100$, where A_0 and A are the initial and final absorbance of solution respectively. Total organic carbon (TOC) measurement was accomplished with a 5000A (Shimadzu) analyzer. The sunlight experiments for all samples were performed simultaneously, using various glass vessels and magnetic stirrers at the same time.

3. Results and discussion

XRD was used to investigate the phase structures and average crystallite size of the Zn_2SnO_4 spinel. Fig. 2 shows typical XRD patterns of Zn_2SnO_4 obtained at 5, 10, 20 and 30 min of 1000 W microwave-assisted irradiation (resulting in 250 °C and 60 bar). According to the XRD patterns, all diffraction peaks can be perfectly indexed to cubic spinel-structured Zn_2SnO_4 (JCPDS Card No. 74-2184). The peaks of the synthesized nanoparticles and those of one standard were the same. No impurities were detected in the synthesized samples. It can be seen that on increasing reaction time the widths of peaks becomes slightly narrow. It is associated with the increase of the crystallite size. The average crystallite size was estimated by applying the Scherrer equation on the highest intensity peak for each sample [18]. The average size changed from 13.32 to 21.57 (as shown in Table 1) when the reaction time increased from 20 to 30 min.

Nitrogen adsorption–desorption isotherms for the Zn_2SnO_4 samples obtained at different reaction times are shown in Fig. 3a. According to the Brunauer–Deming–Deming–Teller (BDDT) classification [19], all the isotherms are of type IV, representing predominantly mesoporous structure characteristics. The mesoporous structure was confirmed by analysis of pore size distribution (Fig. 3b), which shows the spectra of pore diameter with defined maxima in mesoporous region (20 Å < pore diameter < 500 Å) for all the samples. The characterization of mesoporosity was probably due to a variety of accumulated pore voids among particles [20,21]. The pore size distribution curves (Fig. 3b) displayed a unimodal distribution with an average pore size of about 28 and 35 Å (see Table 1) for the samples obtained at 5 and 10 min, respectively, and wide unimodal distribution with an average pore size of about 70 Å for samples obtained at 20 and 30 min. It was found that the textural parameters did not change significantly after 20 min of reaction time (see Table 1). The data concerning pore size shown in Table 1 indicated that the size pore increased with the reaction time, due to the growth of Zn_2SnO_4 crystallites, although the total pore volume was not significantly altered. The particles synthesized at 5 and 10 min presented surface area around 100 $m^2\,g^{-1}$, whereas the samples synthesized at 20 and 30 min presented values of about 60 $m^2\,g^{-1}$ (Table 1). These features are of great importance for catalysis purposes because they allow a greater accessibility of reactant molecules to the catalyst. For the sake of comparison, values of surface area found in literature for the Zn_2SnO_4 oxide prepared from conventional hydrothermal method were 41.24 [22], 41.80 [7] and 62 $m^2\,g^{-1}$ [14]; however these samples were synthesized taking into account a reaction time higher than 12 h.

Photocatalytic tests were carried out using the samples obtained at each synthesis time. Fig. 4 presents the results of degradation percentage of dye as functions of the sunlight irradiation time. Degradation was negligible in the absence of catalyst in the whole period of sunlight irradiation (270 min), indicating that the reduction of dye

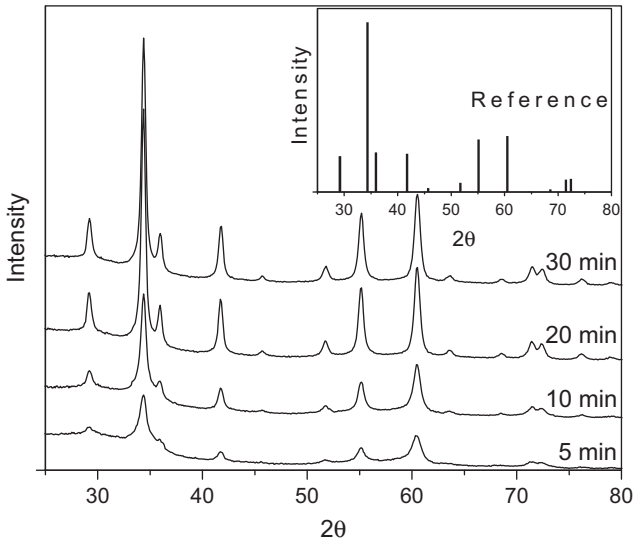

Fig. 2. XRD patterns of the samples prepared at different reaction times, and (inset) reference Zn_2SnO_4 (JCPDS Card No. 74-2184).

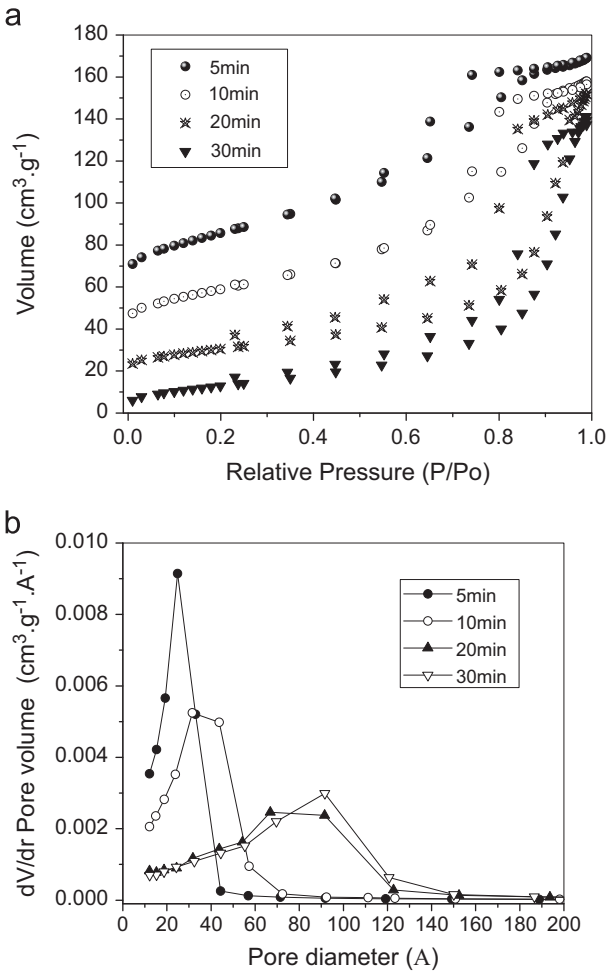

Fig. 3. (a) N_2 ad/desorption isotherms and (b) pore diameter distribution of samples synthesized at different reaction times.

Table 1
Crystallite size, BET surface area and pore parameters of Zn_2SnO_4 particles at different reaction times.

Reaction time (min)	Crystallite size (nm)	Surface area ($m^2\,g^{-1}$)	Total pore volume ($cm^3\,g^{-1}$)	Pore size (Å)
5	13.32	122.93	0.19	28.22
10	16.37	100.32	0.20	35.86
20	19.77	60.45	0.21	67.16
30	20.57	60.25	0.22	70.27

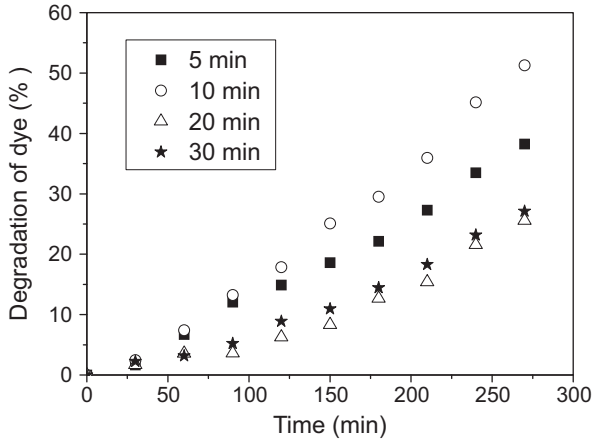

Fig. 4. Degradation of samples obtained at different reaction times.

concentration is due to the photocatalytic activity of Zn_2SnO_4. It is known that when a photon of UV-light radiates the catalyst surface, the conduction band electrons and the valence band holes are generated and then interact with the catalyst surface, where reactive oxygen species such as $OH^{\bullet}$, $HO_2^{\bullet}$, $O_2^{\bullet -}$ radicals are generated [23], leading to the degradation of the dye [24]. Based on the literature reports [25], a possible mechanism for the RR141 dye photodegradation over Zn_2SnO_4 particles irradiated by sunlight can be proposed according to detailed reaction steps as follows:

$$Zn_2SnO_4 + h\nu \rightarrow Zn_2SnO_4\ (e^- + h^+)$$

$$Zn_2SnO_4\ (h^+) + OH^- \rightarrow OH^{\bullet}$$

$$Zn_2SnO_4\ (h^+) + H_2O \rightarrow OH^{\bullet} + H^+$$

$$Zn_2SnO_4\ (e^-) + O_2 \rightarrow O_2^{\bullet -}$$

$$O_2^{\bullet -} + H^+ \rightarrow HO_2^{\bullet}$$

$$Zn_2SnO_4\ (e^-) + H^+ + HO_2^{\bullet} \rightarrow OH^{\bullet} + OH^-$$

$$O_2^{\bullet -} + HO_2^{\bullet} + OH^{\bullet} \text{ or } (h^+) + \text{RR141 dye} \rightarrow \text{degradation products}$$

Based on the above reaction steps, when the Zn_2SnO_4 semiconductor is irradiated by sunlight, electrons (e^-) in the valence band (VB) can be excited to the conduction band (CB) and, simultaneously, the same numbers of holes (h^+) is generated in the VB [25]. The photoinduced holes directly react with RR141 dye or interact with surface-bound H_2O or OH^- to produce the $OH^{\bullet}$ radical species which is a strong oxidant for the mineralization of RR141. Meanwhile, the electrons formed can react with the adsorbed molecular oxygen to yield $O_2^{\bullet -}$. The generated $O_2^{\bullet -}$ then further combine with H^+ to produce $HO_2^{\bullet}$, which can react with the trapped electrons to generate $OH^{\bullet}$ radicals [25]. Thus, the produced reactive species such as $OH^{\bullet}$, $HO_2^{\bullet}$, $O_2^{\bullet -}$ or holes could degrade the RR141 dye.

From Fig. 4, the sample prepared at 10 min degraded 51% of dye after 270 min of sunlight irradiation, and the sample prepared at 5 min degraded 38% in the same reaction time. The samples prepared at 20 and 30 min showed similar activity for dye removal, about 25%. The best photocatalytic activity verified by the sample synthesized at 10 min can be attributed to a number of factors such as high surface area, pronounced mesoporosity of a narrow pore distribution and large pore size.

In order to obtain the kinetics of the reaction the Co/C versus irradiation time were plotted, giving straight lines that indicate zero-order reaction, which are shown in Fig. 5. Zero-order reaction indicates that the rate is independent of reactant concentration, i.e., the amount of dye molecule reacted is proportional to the time. Here "Co" and "C" are the RR141 dye concentrations before and after an irradiation time, respectively. The slopes of these lines correspond to the rate constants of reaction, which were 0.00229, 0.00343, 0.000879 and 0.000982 mg $L^{-1}\,min^{-1}$ for the samples obtained at 5, 10, 20 and 30 min, respectively. The degradation rate of RR141 dye obtained by the photocatalyst prepared at 10 min was 1.5 times greater than the sample prepared at 5 min, and about four times greater than the photocatalysts prepared at 20 and 30 min. The values of the rate constants reflect the conclusions drawn above about the catalysis performances of samples. Zero-order reactions for treatment of aqueous organics have been observed in the presence of TiO_2 [26] and ZnO [27] exposed to artificial UV irradiation, and in the use of $ZnAl_2O_4$ under sunlight [28].

Fig. 6 shows the RR141 dye and TOC removal under sunlight for the Zn_2SnO_4 obtained at 10 min. The results showed about 50% reduction of color after 270 min of sunlight irradiation, whereas the TOC reduction was about 37%. The removal of TOC usually takes longer time after the disappearance of the color [29]. Other researchers also observed that the rate of TOC reduction is remarkably lesser than that of the of dye molecule. Li et al. [25] found that about 77% of TOC still remained in the solution after 5 h of irradiation, whereas rhodamine B dye was almost completely degraded. About 41% reduction of TOC after

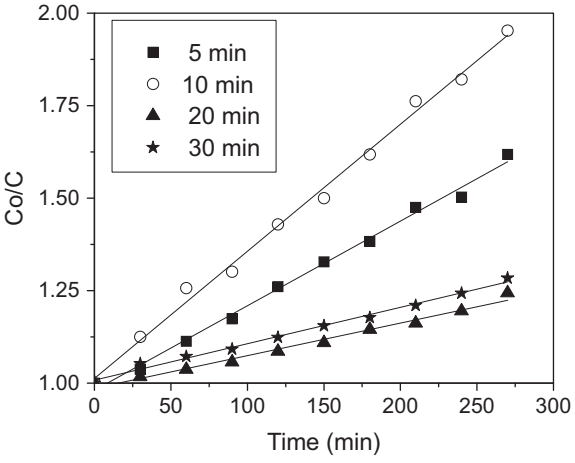

Fig. 5. Photodegradation kinetics of RR141 dye by samples prepared at different reaction times.

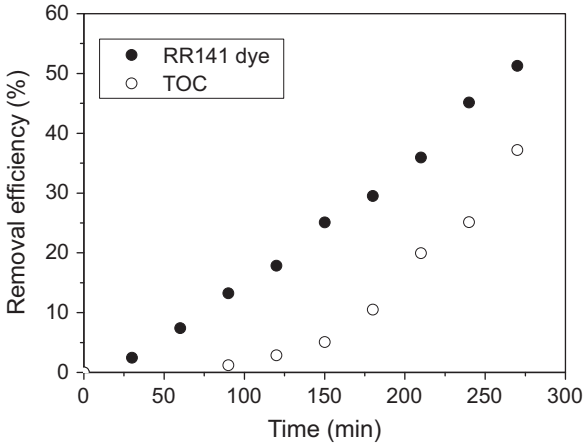

Fig. 6. Comparison of RR141 dye and TOC removal during the course of the photocatalytic degradation with Zn_2SnO_4 prepared at 10 min.

7 h of irradiation using CuO–ZnO photocatalyst for degradation of Acid Red 88 was observed [29]. Also 50% of TOC was removed in 240 min under sunlight in the presence of CeO_2–SnO_2 nanocomposite for the degradation of a leather dye [30]. These results indicated the required long reaction time for complete conversion of the organic dyes to water, carbon dioxide and other inorganic species.

4. Conclusions

Porous Zn_2SnO_4 spinel was prepared successfully by a microwave-assisted hydrothermal route in a short reaction time. This route led to the obtainment of single-phased powders of high quality and crystallinity. The results revealed that all the samples presented mesoporous structure, with a large specific surface area and pore size, leading to the obtainment of materials with important properties for application in the catalysis process. This was confirmed by evaluating the performance of synthesized materials to degrade dye from aqueous solution under sunlight irradiation. The results obtained indicated that the Zn_2SnO_4 particles can be used as an effective photocatalyst for water treatment applications.

Acknowledgments

The authors are grateful to the FIPE Sênior/UFSM for the financial support.

References

[1] W.W. Coffen, Ceramic and dielectric properties of the stannates, Journal of the American Ceramic Society 36 (1953) 207–214.
[2] P. Poix, On some crystallographic and magnetic determinations of oxygen. Compounds having spinel structure, containing tin, titanium, magnesium, zinc and cobalt, Annali di Chimica 10 (1965) 49–79 (Paris).
[3] J.H. Yu, G.M.J. Choi, Selective CO gas detection of Zn_2SnO_4 gas sensor, Journal of Electroceramics 8 (2002) 249–255.
[4] F. Belliard, P.A. Connor, J.T.S. Irvine, Novel tin oxide based anodes for lithium batteries, Solid State Ionics 135 (2000) 163–167.
[5] E.L. Foletto, G.C. Collazzo, M.A. Mazutti, S.L. Jahn, Adsorption of textile dye on zinc stannate oxide: equilibrium, kinetic and thermodynamics studies, Separation Science and Technology 46 (2011) 2510–2516.
[6] C. Wang, X. Wang, J. Fu, Synthesis, characterization and photocatalytic property of nano-sized Zn_2SnO_4, Journal of Materials Science 37 (2002) 2989–2996.
[7] E.L. Foletto, S.L. Jahn, R.F.P.M. Moreira, Hydrothermal preparation of Zn_2SnO_4 nanocrystals and photocatalytic activity in the degradation of leather dye, Journal of Applied Electrochemistry 40 (2010) 59–63.
[8] T. Hashemi, H.M. Al-Allak, J. Illingsworth, A.W. Brinkman, Sintering behavior of zinc stannate, Journal of Materials Science Letters 9 (1990) 776–778.
[9] N. Nikolic, T. Sreckovic, M.M. Ristic, The influence of mechanical activation on zinc stannate spinel formation, Journal of the European Ceramic Society 21 (2001) 2071–2074.
[10] S. Wang, Z. Yang, M. Lu, Y. Zhou, G. Zhou, Z. Qiu, S. Wang, H. Zhang, A. Zhang, Co-precipitation synthesis of hollow Zn_2SnO_4 spheres, Materials Letters 61 (2007) 3005–3008.
[11] Y. Su, L. Zhu, L. Xu, Y. Chen, H. Xiao, Q. Zhou, Y. Feng, Self-catalytic formation and characterization of Zn_2SnO_4 nanowires, Materials Letters 61 (2007) 351–354.
[12] Q.R. Hu, P. Jiang, H. Xu, Y. Zhang, S.L. Wang, X. Jia, W.H. Tang, Synthesis and photoluminescence of Zn_2SnO_4 nanowires, Journal of Alloys and Compounds 484 (2009) 25–27.
[13] J.W. Lee, C.H. Lee, Synthesis of Zn_2SnO_4 anode material by using supercritical water in a batch reactor, Journal of Supercritical Fluids 55 (2010) 252–258.
[14] X. Lou, X. Jia, J. Xu, S. Liu, Q. Gao, Hydrothermal synthesis, characterization and photocatalytic properties of Zn_2SnO_4 nanocrystal, Materials Science and Engineering A 432 (2006) 221–225.
[15] Y. Shen, W. Li, T. Li, Microwave-assisted synthesis of $BaWO_4$ nanoparticles and its photoluminescence properties, Materials Letters 65 (2011) 2956–2958.
[16] Y.Z. Wang, Y. Fu, Microwave-hydrothermal synthesis and characterization of hydroxyapatite nanocrystallites, Materials Letters 65 (2011) 3388–3390.
[17] G.C. Collazzo, E.L. Foletto, S.L. Jahn, M.A. Villetti, Degradation of Direct Black 38 dye under visible light and sunlight irradiation by N-doped anatase TiO_2 as photocatalyst, Journal of Environmental Management 98 (2012) 107–111.
[18] E.L. Foletto, S.L. Jahn, R.F.P.M. Moreira, Synthesis of high surface area $MgAl_2O_4$ nanopowder as adsorbent for leather dye removal, Separation Science and Technology 44 (2009) 2132–2145.
[19] K.S.W. Sing, D.H. Everett, R. Haul, L. Moscou, R.A. Pierotti, J. Rouquerol, T. Siemieniewska, Reporting physisorption data for gas/solid systems, Pure and Applied Chemistry 57 (1985) 603.
[20] Z. Wang, W. Cai, X. Hong, X. Zhao, F. Xu, C. Cai, Photocatalytic degradation of phenol in aqueous nitrogen-doped TiO_2 suspensions with various light sources, Applied Catalysis B: Environmental 57 (2005) 223–231.
[21] G.C. Collazzo, S.L. Jahn, N.L.V. Carreño, E.L. Foletto, Temperature and reaction time effects on the structural properties of titanium dioxide nanopowders obtained via the hydrothermal method, Brazilian Journal of Chemical Engineering 28 (2011) 265–272.
[22] Z. Ai, S. Lee, Y. Huang, W. Ho, L. Zhang, Photocatalytic removal of NO and HCHO over nanocrystalline Zn_2SnO_4 microcubes for indoor air purification, Journal of Hazardous Materials 179 (2010) 141–150.
[23] Z. Chen, D. Li, W. Zhang, Y. Shao, T. Chen, M. Sun, X. Fu, Photocatalytic degradation of dyes by $ZnIn_2S_4$ microspheres under visible light irradiation, Journal of Physical Chemistry C 113 (2009) 4433–4440.
[24] S. Song, Z. Xu, L. He, H. Ying, J. Chen, X. Xiao, B. Yan, Photocatalytic degradation of C.I. direct red 23 in aqueous solutions under UV irradiation using $SrTiO_3/CeO_2$ composite as the catalyst, Journal of Hazardous Materials 152 (2008) 1301–1308.

[25] X. Li, Y. Hou, Q. Zhao, L. Wang, L, A general, one-step and template-free synthesis of sphere-like zinc ferrite nanostructures with enhanced photocatalytic activity for dye degradation, Journal of Colloid and Interface Science 358 (2011) 102–108.
[26] L. Mansouri, L. Bousselmi, A. Ghrabi, Degradation of recalcitrant organic contaminants by solar photocatalysis, Water Science and Technology 55 (2007) 119–125.
[27] W.N.A. Guerra, J.M.T. Santos, L.R.R. Araujo, Decolorization and mineralization of reactive dyes by a photocatalytic process using ZnO and UV radiation, Water Science and Technology 66 (2012) 158–164.
[28] E.L. Foletto, S. Battiston, J.M. Simões, M.M. Bassaco, L.S.F. Pereira, É.M.M. Flores, E.I. Müller, Synthesis of $ZnAl_2O_4$ nanoparticles by different routes and the effect of its pore size on the photocatalytic process, Microporous and Mesoporous Materials 163 (2012) 29–33.
[29] P. Sathishkumar, R. Sweena, J.J. Wu, S. Anandan, Synthesis of CuO–ZnO nanophotocatalyst for visible light assisted degradation of a textile dye in aqueous solution, Chemical Engineering Journal 171 (2011) 136–140.
[30] E.L. Foletto, S. Battiston, G.C. Collazzo, M.M. Bassaco, M.A. Mazutti, Degradation of leather dye using CeO_2–SnO_2 nanocomposite as photocatalyst under sunlight, Water, Air, and Soil Pollution 223 (2012) 5773–5779.